

# Online Solid-Phase Extraction–Inductively Coupled Plasma–Quadrupole Mass Spectrometry with Oxygen Dynamic Reaction for Quantification of Technetium-99

Makoto Matsueda,\* Kayo Yanagisawa, Kazuma Koarai, Motoki Terashima, Kenso Fujiwara, Hironobu Abe, Akihiro Kitamura, and Yoshitaka Takagai\*



Cite This: *ACS Omega* 2021, 6, 19281–19290



Read Online

ACCESS |



Metrics & More



Article Recommendations



Supporting Information

**ABSTRACT:** Quantification of pg/L levels (i.e., 0.6 mBq/L) of radioactive technetium-99 ( $^{99}\text{Tc}$ ) was achieved within 15 min in the presence of isobaric and polyatomic interference sources such as ruthenium-99 ( $^{99}\text{Ru}$ ) and molybdenum hydride ( $^{98}\text{Mo}^1\text{H}$ ) at 3–11 orders of magnitude higher concentrations. Online solid-phase extraction–inductively coupled plasma–quadrupole mass spectrometry (ICP–QMS) with oxygen ( $\text{O}_2$ ) dynamic reaction cell (online SPE–ICP–MS–DRC) was shown to be a thorough automatic analytical system, circumventing the need for human handling. At three stepwise separations (SPE–DRC–Q mass filters), we showed that interference materials allowed the coexistence of abundance ratios of  $1.5 \times 10^{-13}$  and  $1.1 \times 10^{-5}$  for  $^{99}\text{Tc}/\text{Mo}$  and  $^{99}\text{Tc}/\text{Ru}$ , respectively. A classical mathematical correction using the natural isotope ratio of  $^{99}\text{Ru}/^{102}\text{Ru}$  was used to calculate the residues of  $^{99}\text{Ru}$ . Using this optimized system, a detection limit (DL;  $3\sigma$ ) of  $^{99}\text{Tc}$  was 9.3 pg/L (= 5.9 mBq/L) for a 50 mL injection and sequential measurements were undertaken at a cycle of 24 min/sample. For the measurement of a lower concentration of  $^{99}\text{Tc}$ , an AG1-X8 anion-exchange column was used to study 20 L of seawater. Its DL was approximately 1000 times greater than that of previous methods (70.0 fg/L). Thus, this method withstands coexistences of  $5.8 \times 10^{-18}$  and  $3.5 \times 10^{-9}$  for  $^{99}\text{Tc}/\text{Mo}$  and  $^{99}\text{Tc}/\text{Ru}$ , respectively. Spike and recovery tests were conducted for environmental samples; the resulting values showed good agreement with the spike applied.



## INTRODUCTION

Technetium-99 ( $^{99}\text{Tc}$ ) is an artificial radionuclide (half-life:  $2.13 \times 10^5$  y) and pure  $\beta^-$  emitter ( $E_{\text{max}} = 292 \text{ keV}^{1-5}$ ). No stable isotopes of Tc occur in nature; instead, it is highly yielded as a thermal neutron fission product of  $^{235}\text{U}$  (6.1%)<sup>6,7</sup> and  $^{239}\text{Pu}$  (5.9%).<sup>7</sup> The presence of  $^{99}\text{Tc}$  in the environment is thus a result of processes in nuclear energy sources. Discharge from nuclear fuel reprocessing plants in marine environments is its primary source.<sup>8,9</sup> The calculated released  $^{99}\text{Tc}$  amount was about 9 kg of  $^{99}\text{Tc}$  per 1 GW(e) year.<sup>10</sup> Thus, monitoring for administration or regulation is very important. The most stable chemical species of Tc under oxidizing conditions is  $\text{TcO}_4^-$ , which has high mobility in environments. Consequently, the trends of  $^{99}\text{Tc}$  concentration in groundwater around nuclear facilities such as Sellafield<sup>11</sup> and Hanford sites<sup>12</sup> have been monitoring based on the drinking water standards (WHO: 100 Bq/L,<sup>13</sup> EPA (USA): 33 Bq/L<sup>14,15</sup>).

To determine the presence of  $^{99}\text{Tc}$ , inductively coupled plasma–mass spectrometry (ICP–MS) has been widely utilized owing to its high sensitivity, rapidity, and high throughput instead of traditional radiometric analytical methods such as low-background  $\beta$  counter or liquid scintillation. ICP–MS analyses require the chemical separation

of  $^{99}\text{Tc}$  from other coexisting nuclides to prevent isobaric and polyatomic interferences. Although the generation of isobars is possible through polyatomic ions (e.g.,  $^{40}\text{Ca}^{18}\text{OH}^{40}\text{Ar}$ ,  $^{43}\text{Ca}^{16}\text{O}^{40}\text{Ar}$ ,  $^{51}\text{V}^{16}\text{O}_3$ ,  $^{59}\text{Co}^{40}\text{Ar}$ ,  $^{62}\text{Ni}^{37}\text{Cl}$ ,  $^{63}\text{Cu}^{36}\text{Ar}$ ,  $^{64}\text{Zn}^{35}\text{Cl}$ ,  $^{87}\text{Rb}^{12}\text{C}$ , and  $^{87}\text{Sr}^{12}\text{C}$ ),<sup>16,17</sup> the primary isobaric and polyatomic interferences are often found around  $m/z$  99 due to  $^{98}\text{Mo}^1\text{H}$  and  $^{99}\text{Ru}$ . The occurrence rates of these interferences have been reported as the  $^{98}\text{MoH}/\text{Mo}$  ratio is on the order of  $10^{-5}$ – $10^{-6}$  for ICP–single quadrupole MS (ICP–QMS)<sup>18</sup> and ICP–sector field MS (ICP–SFMS),<sup>19</sup> arising from the 12.76% of natural Ru that occurs as  $^{99}\text{Ru}$ . Other typical major interferences are caused by mass-spectral overlapping problems arising from peak tailing of excess amounts of  $^{98}\text{Mo}$ . Such peak tailing appears at  $m/z$  99 due to the abundance of Mo (natural isotopes, i.e.,  $(m/z\ 99)/\text{Mo} = 10^{-6}$ – $10^{-7}$ ).<sup>16,20,21</sup> To overcome

Received: May 26, 2021

Accepted: June 25, 2021

Published: July 16, 2021



these interferences, the separation efficiency (discrimination) demands values exceeding  $3.4 \times 10^{-9}$  and  $3.1 \times 10^{-2}$  for  $^{99}\text{Tc}/\text{Mo}$  and  $^{99}\text{Tc}/\text{Ru}$ , respectively, shown in Table S1 in the Supporting Information (SI). The  $^{99}\text{Tc}$  values were observed at monitoring points in the Sellafield and Hanford sites (less than 6 mBq/L, equivalent to 9.5 pg/L).<sup>11,12</sup> Meanwhile, the Ru and Mo concentrations in typical environmental water are 0.5–1.5 ng/L and 30 ng/L–13.9 mg/L, respectively.<sup>22–24</sup> Regarding Mo concentrations in freshwater, the concentrations are significantly different in the water type, sampling location, and depth of sampling.<sup>22</sup> Numerous studies have addressed the utilization of solid-phase extraction (SPE) approaches as a means to separate and enrich  $^{99}\text{Tc}$  prior to analysis via ICP–QMS. In particular, the commercially available TEVA resin has been widely used as the SPE resin for separating  $^{99}\text{Tc}$  prior to ICP–MS analysis.<sup>25–30</sup> The typical protocol of TEVA resin requires acidic conditions (0.05–0.1 M  $\text{HNO}_3$ ) in the adsorption of  $^{99}\text{Tc}$  onto the resin; in contrast, highly acidic conditions (6.5–8 M) are required for its elution.

Online SPE–ICP–MS is an automatic sequential analytical technology characterized by good repeatability and high-speed data acquisition. By virtue of these advantages, coupled SPE–ICP–MS systems have been widely employed to monitor environmental radioactivity.<sup>31–48</sup> For radionuclide analysis, this coupled system provides radiological protection to operators by suppressing the exposure dose. For example, the system is useful for monitoring radioactivity during the decommissioning of nuclear power plants. In spite of this, relatively few studies have reported online SPE (TEVA resin)–ICP–MS methods for  $^{99}\text{Tc}$  analysis.<sup>26,29,30,49</sup> The primary reasons for this can be attributed to the difficulties involved in the direct introduction of eluate into ICP–MS (after SPE). Numerous challenges have been identified. (i) While all reported  $^{99}\text{Tc}$  analyses of online SPE–ICP–MS used TEVA resin as the SPE column, the final solution eluted from the SPE column was obtained as a highly acidic solution (6.5–8.0 M  $\text{HNO}_3$ ). This solution often damages parts of ICP–MS, causing Mo (interference element) to leak from the material of the ICP–MS [note: see the online SPE of  $^{99}\text{Tc}$  in the Results and Discussion section]. To avoid this problem, the eluate after SPE (TEVA) must be collected before introduction into the ICP–MS; thus, reparation such as evaporation, dryness, and replacement is required to ensure that a milder solution is injected into the ICP–MS. Consequently, it is necessary to remedy inefficiency via an automatic system of  $^{99}\text{Tc}$  analysis without human handling. (ii) Stricter separation of Mo and Ru from  $^{99}\text{Tc}$  is required. Treatments requiring a large volume of the sample solution are necessary to measure very low concentrations of  $^{99}\text{Tc}$ . A single-step separation using only SPE is not sufficient,<sup>50</sup> and it is difficult to measure the background control on enriched concentrations of Mo and Ru. In other words, the DL of  $^{99}\text{Tc}$  based on ICP–MS analysis depends on the abundance ratios of  $^{99}\text{Tc}/\text{Mo}$  and  $^{99}\text{Tc}/\text{Ru}$ . To improve the sensitivity of  $^{99}\text{Tc}$ , it is crucial to suppress (i.e., to reduce the value of) the allowed abundance ratios of  $^{99}\text{Tc}/\text{Mo}$  and  $^{99}\text{Tc}/\text{Ru}$ .<sup>51</sup> This requires a larger volume of sample to be preconcentrated in a smaller volume and directly injected into the ICP–MS system (either online or offline).

In this study, we present online automation of the SPE–ICP–MS system requiring no human handling by applying a combination of three separations: (i) online SPE using TK201, (ii)  $\text{O}_2$  dynamic reaction cell (DRC), and (iii) quadrupole mass filtering. Although the dynamic reaction cell (DRC) is an

important technique for the separation of isobaric interference, no previous studies have addressed its use in separating Mo and  $^{99}\text{Tc}$ . Combination effects on the quantification of  $^{99}\text{Tc}$  are thus evaluated as part of the present study. In addition, the proposed method can allow additional combinations between offline preconcentration methods. Thus far, no study has considered ultralow abundance ratios of  $^{99}\text{Tc}/\text{Mo}$  and  $^{99}\text{Tc}/\text{Ru}$  in the automated  $^{99}\text{Tc}$  analysis. Furthermore, spike and recovery tests for environmental water samples (e.g., groundwater, river water, deep pond mineral water, seawater, and concentrated seawater) were investigated.

## EXPERIMENTAL SECTION

**Apparatus.** The online SPE–ICP–MS used in this study comprised the following instruments: a NexION 300X ICP–MS equipped with a DRC (PerkinElmer, Inc., Shelton, CT), a U5000AT+ ultrasonic nebulizer (USN; Teledyne CETAC Technology, NE), an FIAS400 flow injection system (PerkinElmer) featuring specially fabricated double eight-way switching valves, and an S10 autosampler (PerkinElmer). Ultrapure (>99.999%) gases were used for the DRC as collision/reaction gases ( $\text{O}_2$ , He,  $\text{NH}_3$ ,  $\text{CH}_4$ ), and argon ion source was used as the mixed-gas plasma ( $\text{N}_2$ ).

**Reagents and Preparation.** A radioactive  $^{99}\text{Tc}$  stock solution (50 Bq/g (= 79 ng/g); radioactive purity >99%) obtained from Kaken Corporation Ltd. (Ibaraki, Japan) was diluted to the required concentration. Solution mixtures of 70 elements were prepared by mixing XSTC series #1, #7, #8, and #13 standard stock solutions of metal ion mixtures (stable isotopes; concentration: 10 mg/L; SPEX Certiprep, Inc., Metuchen, NJ). Single-element stock solutions (1000 mg/L; atomic absorption spectrometry grade) were obtained from the FUJIFILM Wako Pure Chemical Co. (Osaka, Japan). Concentrated  $\text{HNO}_3$  (ultrapure grade, 69 w/w%) was obtained from Kanto Chemical Co., Inc. (Tokyo, Japan). Ultrapure water (18.2 M $\Omega$ ·cm) was obtained from a PURELAB Ultra purifier (ELGA, Bucks, U.K.). SPE powders (440 mg) of TK201 resin (particle diameter: 100–150  $\mu\text{m}$ ; TRISKEM International, Bruz, France) were packed half amounts into two empty polyetheretherketone (PEEK) columns (PerkinElmer; 3.5 mm I.D., 50 mm long). A strong anion exchanger, AG1-X8 (11.7 g), was used as the offline preconcentration resin (particle diameter: 100–150  $\mu\text{m}$ ; quaternary ammonium groups; BioRad Laboratories Inc. Hercules, CA) and packed into an empty polypropylene (PP) column (PerkinElmer; 18 mm I.D., 55 mm long). All other reagents, which were of analytical grade, were obtained from the FUJIFILM Wako Pure Chemical Corporation (Osaka, Japan) and were used without further purification unless otherwise noted.

**Sample Collection and Pretreatment.** *Preparation of Environmental Samples.* River water, groundwater, deep pond mineral water, and seawater were collected in Fukushima, Ibaraki, and Kumamoto prefectures in Japan. A reference material, IAEA-443 Irish seawater, with an information value of  $^{99}\text{Tc}$  was used to evaluate the proposed method. These samples were filtered using a hydrophilic poly(tetrafluoroethylene) (PTFE) polymer membrane filter (0.45  $\mu\text{m} \times 47 \text{ mm}$ ). Hundred milliliters of sample volume was prepared at 0.7 M  $\text{HNO}_3$  aq. sol. via an appropriate serial dilution of ultrapure  $\text{HNO}_3$  before ICP–MS analysis. The injection volume of the sample was 50 mL (as 0.7 M  $\text{HNO}_3$  aq. sol.).

### Offline Preconcentration for Lower Concentration of Environmental Samples.

As an additional pretreatment, AG1-X8 strong anion exchanger was used before injection into the system following the procedures reported in the literature.<sup>52,53</sup> Four milliliters of 100 mg/L rhenium (Re) was spiked into 40 L of seawater sample as a tracer [note: in this case, the recoveries between Tc and Re well corresponded. The capacity was commercially reported as 1.2 meq/mL (equal to 32 g/L as Re)]. Samples (40 L) were passed through the AG1-X8 anion-exchange column at a flow rate of 100 mL/min to enable the adsorption of <sup>99</sup>Tc using a diaphragm pump (SIMDOS 10 FEM 1.10 TT. 18RC2, KNF Neuberger, Inc., Freiburg, Germany), after which the column was cleaned with 200 mL of 0.5 M HNO<sub>3</sub> at the same flow rate. <sup>99</sup>Tc (with Re) was eluted by passing 50 mL of 12 M HNO<sub>3</sub> into the column. The eluted solution was heated using a hot plate at 100 °C until completely dry; then, it was diluted using 20 mL of 0.7 M HNO<sub>3</sub> (i.e., a preconcentration factor of 2003 times (from 40.055 L to 20 mL)). An aliquot (10.0 mL) of the condensed seawater was injected into the proposed system. To monitor the recovery of <sup>99</sup>Tc, concentrations of the Re tracer were measured before and after preconcentration using the AG1-X8 anion-exchange column. The recovery rate (R%) was calculated as follows

$$R\% = \frac{C_f V_f}{C_i V_i} \times 100 \quad (1)$$

where  $C_i$  and  $C_f$  are the initial and final concentrations of Re, respectively, and  $V_i$  and  $V_f$  are the initial and final (eluate) volumes, respectively.

**Autosequential Online SPE–ICP–MS–DRC System.** The scheme of the proposed SPE–ICP–MS–DRC system is shown in Figure 1, and the experimental parameters are shown in Table S2 in the SI. Two flow lines controlled by automation switching valves were arranged in the system (Figure 1). Figure 1A shows valve position #1, which influences the online SPE step (red flow line) and the clean-up line (black flow line). Fifty milliliters of a sample solution containing <sup>99</sup>Tc (0.7 M HNO<sub>3</sub> aq. sol.) was injected into the proposed system via an autosampler (red line). After injection, the sample passed through the SPE column via pump #2 at a flow rate of 5.0 mL/min. During the sample flow into the column, <sup>99</sup>Tc was adsorbed onto the resin, while unadsorbed elements were discharged into the drain. Then, the column was rinsed with approximately 33 mL of 0.7 M HNO<sub>3</sub> (flow rate: 5.0 mL/min). During the abovementioned steps (i.e., sample injection, SPE step, and rinsing), 3.0 M HNO<sub>3</sub> flowed inside the other flow line (i.e., the black line), where it was merged with 100 ng/L rhodium (Rh) aq. sol. (0.4 M HNO<sub>3</sub>) as an internal standard (ISTD) via pump #1 at a flow rate of 1.0 mL/min (3.0 M HNO<sub>3</sub>: ISTD = 13:1). The resulting mixture was introduced into ICP–MS via the USN. After all sample volumes had passed through the SPE column, the valve was switched from position #1 to position #2.

Figure 1B (valve position #2) shows the steps involved in the elution of <sup>99</sup>Tc and its measurement via ICP–MS (red flow line). The eluate (3.0 M HNO<sub>3</sub>) was passed through the SPE column at a flow rate of 2.0 mL/min, and the adsorbed <sup>99</sup>Tc was eluted. The elution shown by the red line was merged with the ISTD sol. in the black line (0.16 mL/min), after which <sup>99</sup>Tc was introduced into the ICP–MS via the USN. During elution and measurement via ICP–MS, any liquid flowing

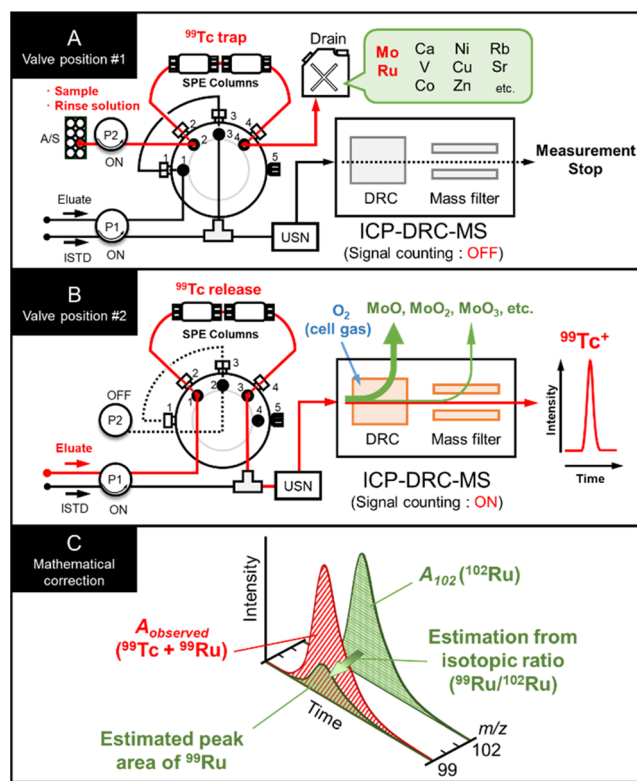


**Figure 1.** Scheme of the online SPE–ICP–MS–DRC system: (A) valve position A representing the loading of a sample to the column (<sup>99</sup>Tc adsorption) and rinsing; (B) valve position #B representing the elution of <sup>99</sup>Tc from the SPE column and its introduction into the ICP–MS via the USN. Eluted nuclides are ionized in plasma and then exposed to O<sub>2</sub> gas in the DRC. Surviving <sup>99</sup>Tc is filtered via QMS, and the isolated <sup>99</sup>Tc is detected at  $m/z$  99. The flow signal chromatographic peak is thus obtained; (C) mathematical correction of measurement values to avoid isobaric interference from <sup>99</sup>Ru using the natural isotopic ratio of Ru (<sup>99</sup>Ru/<sup>102</sup>Ru: mass bias was controlled).

along the black dotted line was retained until the next sample analysis. Following its introduction into the ICP–MS, the remaining Mo (and other high-valence metal ions) reacted with O<sub>2</sub> in the DRC and interference nuclides (i.e., the tailing from <sup>98</sup>Mo and polyatomic ions such as <sup>98</sup>MoH) were separated by the QMS filter. For the ISTD, the intensities of <sup>99</sup>Tc as target ion are divided by the intensities of <sup>115</sup>In. For quantification, a calibration curve (0.0, 0.1, 0.2, 0.5 ng/L) was prepared using a set of standard solutions vs peak areas (signal integration) of <sup>99</sup>Tc. Signal integration was conducted by Microsoft Excel. Monitoring ions at  $m/z$  98, 99, 102, and 103 were measured and identified as <sup>98</sup>Mo, <sup>99</sup>Tc, <sup>102</sup>Ru, and <sup>103</sup>Rh, respectively. In addition, the cell pass voltage was adjusted using natural Mo isotopes, and all isotopes of relative abundance for Mo were adjusted in the mass spectrometer.

**Mathematical Correction of Measurement Values.** To avoid isobaric interference from <sup>99</sup>Ru, the classical mathematical correction using the isotopic ratio of Ru (<sup>99</sup>Ru/<sup>102</sup>Ru) was conducted following previous protocols<sup>21</sup> (as shown in Figure 1C). The isotopic abundance ratio of <sup>99</sup>Ru/<sup>102</sup>Ru was actually measured using a standard solution (100 μg/L). Overlapping <sup>99</sup>Ru counts on the observed peak ( $m/z$  99) were eliminated by the following eq 2



$$\text{net } A_{99}(\text{cps}) = A_{\text{observed}} - \frac{{}^{99}\text{Ru}}{{}^{102}\text{Ru}} \times A_{102} \quad (2)$$

where  $A_{\text{observed}}$ ,  $A_{102}$ , and net  $A_{99}$  correspond to the peak areas of  $m/z$  99 observed via ICP–MS,  $m/z$  102 from  ${}^{102}\text{Ru}$ , and the net value given by  ${}^{99}\text{Tc}$ , respectively. The value  ${}^{99}\text{Ru}/{}^{102}\text{Ru}$  is mass-biased via ICP–MS.

The DL for online SPE–ICP–MS was calculated from the slope of the calculation curve and standard deviation ( $3\sigma$ ) of the blank sample. With additional offline preconcentration (in this case, ion exchanger), the DL was calculated as follows

$$\text{DL}_{\text{total}} = \text{DL} \times \frac{C_i}{C_f} \quad (3)$$

## RESULTS AND DISCUSSION

As preliminary confirmation, a significant difference between the background noise signal at  $m/z$  99 (typically  $24.7 \pm 4.8$  cps in 0.4 M  $\text{HNO}_3$  aq. sol.) and the signal intensity of the target was confirmed by injecting 10 metal ions (Mo: 10 mg/L, Ru: 100 ng/L, Ca: 500 mg/L, V: 100  $\mu\text{g/L}$ , Co: 10  $\mu\text{g/L}$ , Ni: 100  $\mu\text{g/L}$ , Cu: 100  $\mu\text{g/L}$ , Zn: 100  $\mu\text{g/L}$ , Rb: 10 mg/L, Sr: 10 mg/L) into an ICP–MS. When 10 mg/L Mo and/or 100 ng/L Ru solutions were individually injected into the ICP–MS via the cyclonic spray chamber, the signal intensity at  $m/z$  99 was both increased and disturbed by the presence of these elements ( $2678 \pm 211$  and  $875 \pm 30$  cps for  ${}^{98}\text{Mo}^1\text{H}$  and  ${}^{99}\text{Ru}$ , respectively). The other eight elements showed no impact on the intensity ( $m/z$  99); therefore, we assumed that Mo and Ru were the primary sources of interference. When 0.27 mg/L of Mo or 3.7 ng/L of Ru is individually measured, the  $m/z$  99 counts (>background level) were generated. In other words, without any separation, interference problems noted around  $m/z$  99 were greater than the intensity ratios  $2.7 \times 10^{-5}$  and  $3.7 \times 10^{-12}$  for  $(m/z$  99)/Mo and  $(m/z$  99)/ ${}^{99}\text{Ru}$ , respectively. The intensity of Mo related to primary  ${}^{98}\text{Mo}^1\text{H}$  and peak tailing from excess amounts of  ${}^{98}\text{Mo}$  is described in the Separation of Mo by DRC section.

**Online SPE of  ${}^{99}\text{Tc}$ .** By contract with TEVA,<sup>51</sup> a commercially available TK201 resin<sup>54</sup> was used to capture  ${}^{99}\text{Tc}$  under neutral pH and release  ${}^{99}\text{Tc}$  at concentrations of less than 3.0 M  $\text{HNO}_3$ . The two resins, TEVA and TK201, were evaluated; Figure S1 in the SI shows the adsorbability of 65 elements (10 mL of 100  $\mu\text{g/L}$  each element). When the mixture solution passed through the SPE column, the recoveries were calculated by the difference of the concentration. Both showed effective adsorption of  ${}^{99}\text{Tc}$  on the SPE column and the separation of Mo and Ru. The recovery rates (for 10 mL eluate; relative standard deviation, RSD) were 94.9% ( $\pm 1.7\%$ ), 0.86% ( $\pm 0.01\%$ ), and 0.37% ( $\pm 0.02\%$ ) for  ${}^{99}\text{Tc}$ , Mo, and Ru in the TK201 resin, respectively. In contrast, the TEVA resin exhibited values of 104.6% ( $\pm 0.56\%$ ), 0.13% ( $\pm 0.02\%$ ), and 0.67% ( $\pm 0.03\%$ ) for  ${}^{99}\text{Tc}$ , Mo, and Ru, respectively. These results indicate that the TK201 resin (without DRC) discriminates Mo from Tc in the ratios of  $>9.1 \times 10^{-3}$  and  $>3.9 \times 10^{-3}$  for  ${}^{99}\text{Tc}/\text{Mo}$  and  ${}^{99}\text{Tc}/\text{Ru}$ , respectively. These values were, however, insufficient to separate  ${}^{99}\text{Tc}$  from natural Ru and Mo in environmental waters. Water sample analysis (without any pretreatment) around nuclear facilities requires values below  $3.4 \times 10^{-9}$  and  $3.1 \times 10^{-2}$  for  ${}^{99}\text{Tc}/\text{Mo}$  and  ${}^{99}\text{Tc}/\text{Ru}$ , respectively.

On the other hand, the elution of  ${}^{99}\text{Tc}$  from the columns requires acid solution as the eluate. The TEVA resin used a higher concentration (8.0 M) of  $\text{HNO}_3$ , whereas TK201<sup>56</sup> required a relatively low concentration (3.0 M). The direct injection of samples dissolved in higher concentrations of  $\text{HNO}_3$  into ICP–MS can result in damage to certain interfaces and metallic parts of the ICP–MS (e.g., the sampling cone and/or skimmer cone). For two different concentrations of  $\text{HNO}_3$  solutions (each 5 mL, with concentrations of 3.0 and 8.0 M) in contact with a Ni sampling cone (i.e., a part of the QMS) for 90 min, the resulting concentrations of Mo and Ru increased to 9.5 mg/L, 244.2  $\mu\text{g/L}$ , and 67.3 g/L for Mo, Ru, and Ni, respectively (for 8.0 M  $\text{HNO}_3$ ); in contrast, the values for 3.0 M  $\text{HNO}_3$  were 4.5 mg/L, 56.8  $\mu\text{g/L}$ , and 20.3 g/L for Mo, Ru, and Ni, respectively. To suppress damage of metallic parts and leakages of the interference material from these parts (i.e., to suppress background counts), a lower concentration of  $\text{HNO}_3$  solution is preferable. These results showed that the TK201 resin was preferable over TEVA in the online  ${}^{99}\text{Tc}$  SPE column.

Achieving a DL of monitoring level (less than 6 mBq/L), it is necessary to enrich more  ${}^{99}\text{Tc}$  into the SPE column by increasing the sample volume. However, the SPE single column with the TK201 resin (220 mg) had lost  ${}^{99}\text{Tc}$  in proportion to the passed sample/rinse volume. Therefore, the inline style double SPE columns (440 mg) were employed to maintain the recovery rate. Figure S2A in the SI shows that the adsorption rate of  ${}^{99}\text{Tc}$  (1.0  $\mu\text{g/L}$ , 10–100 mL) maintained over 99% up to 100 mL sample volume. Figure S2B in the SI shows the recovery rate of  ${}^{99}\text{Tc}$ , Mo, and Ru corresponding to rinse volume (after loading 50 mL sample). The final recovery rates were 99.6, 0.029, and 0.022% for  ${}^{99}\text{Tc}$ , Mo, and Ru, respectively (sample: 50 mL, rinse: 30 mL). The double SPE columns enhanced the sensitivity of  ${}^{99}\text{Tc}$  approximately five times, and the abundance ratios indicated  $2.9 \times 10^{-4}$  and  $2.2 \times 10^{-4}$  for  ${}^{99}\text{Tc}/\text{Mo}$  and  ${}^{99}\text{Tc}/\text{Ru}$ , respectively.

**Separation of Mo by DRC.** To remove the small amount of residual Mo, DRC separations were investigated using typical gases ( $\text{O}_2$ ,  $\text{NH}_3$ , He, and  $\text{CH}_4$ ) for the separation step. To confirm the effect of DRC, 1.0  $\mu\text{g/L}$   ${}^{99}\text{Tc}$  and a  $10^4\times$  excess concentration (10 mg/L) of Mo (dissolved in 0.4 M  $\text{HNO}_3$ ) were individually injected into the ICP–MS via the cyclonic spray chamber, which is connected with a microflow-type nebulizer without an online SPE column. Figure S3 in the SI shows the effects of several gases on the DRC. Numerous studies have addressed the utilization of such an  $\text{O}_2$  gas-loading approach as a means to separate Mo,<sup>55,56</sup> however, the quantitative removal of Mo via different gas species has not yet been investigated. Oxygen was found to be most effective in the removal of Mo (i.e.,  $m/z$  98 and 99 for  ${}^{98}\text{Mo}$  and  ${}^{98}\text{Mo}^1\text{H}$ , respectively) while maintaining the intensity of  ${}^{99}\text{Tc}$ . The intensities of  ${}^{98}\text{Mo}$  and  ${}^{98}\text{Mo}^1\text{H}$  decreased to background levels, as shown in Figure S3A,B in the SI. In contrast, the intensity of  ${}^{99}\text{Tc}$  was maintained against  $\text{O}_2$  exposure (Figure S3C in SI). Other gases (He,  $\text{CH}_4$ , and  $\text{NH}_3$ ) were found to be insufficient for the removal of excess amounts of Mo, although slight decreases were observed in  $m/z$  98 and 99. The major differences between  $\text{O}_2$  and these gases result from oxidation (addition of O atoms) and the simple collision effect.<sup>57</sup> In addition, the  $10^1$ – $10^2$  intensity of Tc decreased under exposure to  $\text{NH}_3$  and He (Figure S3C), whereas Tc survived under  $\text{O}_2$  and  $\text{CH}_4$ . It seems that the charge transfer occurred notably under  $\text{NH}_3$ , which has the lowest ionization potential

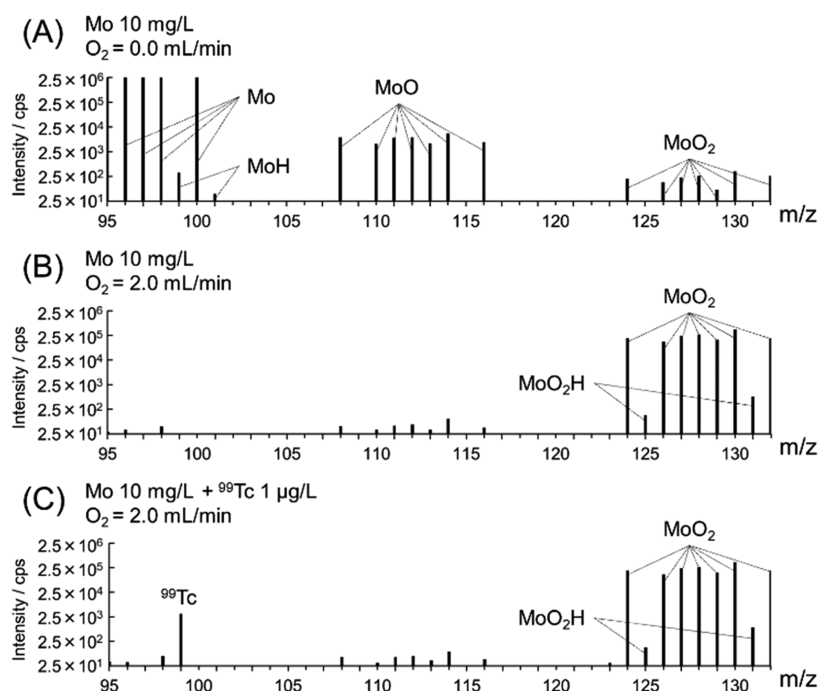


**Figure 2.** Mass spectra of the Mo-standard (Mo-STD) solution with and without  $O_2$  reaction in DRC. (A) 10 mg/L Mo-STD without DRC; (B) 10 mg/L Mo-STD via DRC ( $O_2$ : 2 mL/min); and (C) 1  $\mu\text{g/L}$   $^{99}\text{Tc}$  coexisting with 10 mg/L Mo-STD via DRC ( $O_2$ : 2 mL/min). Experimental conditions: ICP–MS measurement was conducted via a cyclonic spray chamber connected to a microflow-type nebulizer.

(10.16, 12.07, and 12.6 eV for  $\text{NH}_3$ ,  $O_2$ , and  $\text{CH}_4$ , respectively),<sup>58,59</sup> and high pressure of He excluded Tc with increasing the number of collisions.<sup>60</sup>

Figure 2A shows the mass spectrum of Mo without the  $O_2$  reaction in DRC. Mo has seven natural isotopes (relative abundances): 92 (14.84%), 94 (9.25%), 95 (15.92%), 96 (16.68%), 97 (9.55%), 98 (24.13%), and 100 (9.63%). Despite no isotope with mass number 99 occurring in nature, an obvious signal was confirmed on the target position ( $m/z$ ) of 99, and many signals were observed over 100. These originate from  $^{98}\text{Mo}^1\text{H}$  and polyoxides of Mo (such as MoO and  $\text{MoO}_2$ ; formation of Mo polyoxometalate is well known and detected by ICP–MS<sup>59</sup>). In addition, the mass spectrometric signal tailing arising from excess Mo (primary source:  $^{98}\text{Mo}^+$ ) may be observed over  $m/\Delta m = \text{approx. } 10^6$ .<sup>16,20</sup> Figure 2B shows the mass spectrum of Mo with the  $O_2$  reaction in DRC. Mo signals are observed to shift to higher mass numbers stemming from  $\text{MoO}_2$  and  $\text{MoO}_2\text{H}$ . The interfered species ( $^{98}\text{Mo}^+$  and  $^{98}\text{Mo}^1\text{H}^+$ ) disappeared, and the resulting position ( $m/z$ ) of 99 has no features. Figure 2C shows the mass spectrum of 1  $\mu\text{g/L}$   $^{99}\text{Tc}$  in the presence of a  $10^4\times$  excess concentration of Mo (10 mg/L) with  $O_2$  reactions in DRC, demonstrating that the resulting signal of  $^{99}\text{Tc}$  survives.

The volume (flow rate) of  $O_2$  influenced the intensity of Mo, whereas the intensity of  $^{99}\text{Tc}$  remained constant within the entire volume of  $O_2$ , as shown in Figure 3A. In the absence of  $O_2$  (0 mL/min), the variety of Mo species such as  $^{98}\text{Mo}^+$  ( $m/z$  98),  $^{98}\text{Mo}^1\text{H}^+$  ( $m/z$  99),  $^{98}\text{Mo}^{16}\text{O}^+$  ( $m/z$  114), and  $^{98}\text{Mo}^{16}\text{O}_2^+$  ( $m/z$  130) existed natively. Among them,  $^{98}\text{Mo}^+$ ,  $^{98}\text{Mo}^1\text{H}^+$ ,  $^{98}\text{Mo}^{16}\text{OH}^+$ , and  $^{98}\text{Mo}^{16}\text{O}^+$  decreased logarithmically with increasing  $O_2$ . A small amount of  $^{98}\text{Mo}^{16}\text{O}^+$  and  $^{98}\text{Mo}^{16}\text{OH}^+$  survived at higher  $O_2$  flow rates; otherwise, di- and trioxide ions and their related hydrated ions (i.e.,  $^{98}\text{Mo}^{16}\text{O}_2^+$ ,  $^{98}\text{Mo}^{16}\text{O}_3^+$ ,  $^{98}\text{Mo}^{16}\text{O}_2\text{H}^+$ , and  $^{98}\text{Mo}^{16}\text{O}_3\text{H}^+$ , and others), which are thermodynamically stable with a binding

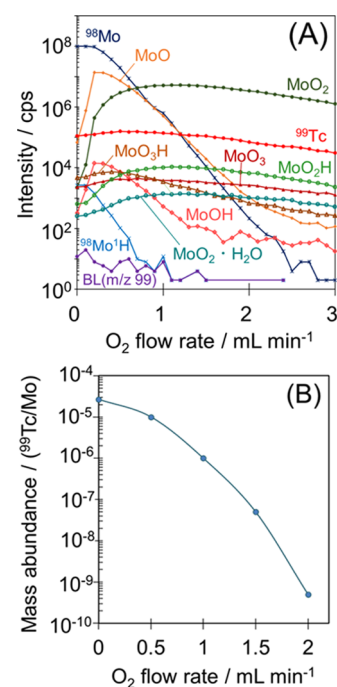


**Figure 3.** Effect of  $O_2$  flow rate (DRC) on (A) the variation of Mo species and (B) the allowed coexistence of Mo with  $^{99}\text{Tc}$ . Experimental conditions: both (A) and (B) were the absence of SPE; they only used DRC. (A) 1.0 ng/L  $^{99}\text{Tc}$  sol with 10 mg/L Mo sol. and (B) 1.0 ng/L  $^{99}\text{Tc}$  with different orders of magnitude of Mo (0.1–500 mg/L). While maintaining the precision of quantification ( $1.00 \pm 0.2$  ng/L (20%)) for  $^{99}\text{Tc}$ , the allowed maximum  $^{99}\text{Tc}/\text{Mo}$  ratios (amount) were plotted in each  $O_2$  flow rate.

energy of 144 kcal/mol for  $\text{MoO}_2^+$ ,<sup>61</sup> were present within the entire flow rate of  $O_2$ . Under He gas atmospheres,<sup>61,62</sup> the presence of higher oxides, for example,  $^{98}\text{Mo}^{16}\text{O}_4^+$ ,  $^{98}\text{Mo}^{16}\text{O}_5^+$ ,

and  $^{98}\text{Mo}^{16}\text{O}_6^+$ , was reported; however, these were not detected in the DRC of the ICP–MS. The oxidation process of Mo in He atmospheres depends on the concentration of  $\text{O}_2$ ,<sup>62</sup> similar phenomena control the mechanisms of oxidation in the DRC. In contrast, the intensity of  $^{99}\text{Tc}$  (1.0  $\mu\text{g/L}$ ) varied only 1% from the initial intensity under  $\text{O}_2$  flows of up to 1.5 mL/min. When 1.00 ng/L  $^{99}\text{Tc}$  solutions with different amounts of Mo were measured, the quantitative tolerance of  $^{99}\text{Tc}$  (1.00  $\pm$  0.2 ng/L) was found to depend on the flow rate of  $\text{O}_2$ , as shown in Figure 3B. Consequently, the DRC (without online SPE) discriminated  $5 \times 10^{-10}$  for  $^{99}\text{Tc}/\text{Mo}$  under the condition of a 2.0 mL/min  $\text{O}_2$  flow rate; i.e., it means that the count rate of Mo in  $m/z$  99 corresponds to only  $5 \times 10^{-10}$  of  $^{99}\text{Tc}$ . Otherwise, the DRC was not effective for removing  $^{99}\text{Ru}$  (see Figure S4).

**Mathematical Correction of  $^{99}\text{Tc}$  from  $^{99}\text{Ru}$ .** To avoid interference from small amounts of  $^{99}\text{Ru}$  residues, a mathematical correction<sup>21</sup> was applied following the protocol presented in the Experimental Section. The isotope abundance ratio of  $^{99}\text{Ru}/^{102}\text{Ru}$  was 0.388 obtained from the measurement result of Ru standard (100  $\mu\text{g/L}$ ), and the concentration of Ru after SPE was only 0.022% of its initial concentration. The measurement error of  $A_{102}$  (for  $^{102}\text{Ru}$ ) was within 5%. Overlapping  $^{99}\text{Ru}$  counts on the observed peak ( $m/z$  99) were successfully eliminated because the solution with nonspiked  $^{99}\text{Tc}$  showed a signal equal to the background signal after correction. The correction satisfied the condition under which a significant difference between the intensities of net  $A_{99}$  and  $A_{\text{Ru}-99}$  (i.e.,  $0.388 \times A_{\text{Ru}-102}$ ) that is greater than the value of the measurement error of Ru (5%) is required: net  $A_{99} > 1.05 (0.388 \times A_{\text{Ru}-102})$ . Therefore, the coexistence ratio (mass abundance) for  $^{99}\text{Tc}/\text{Ru}$  was 0.05 (i.e., 5/100).

**Autosequential Online SPE–DRC–ICP–MS System.** Figure 4 shows the chromatographic peaks ( $m/z$  99) obtained

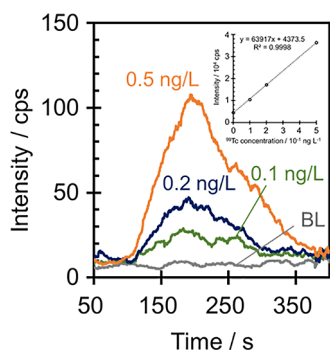


**Figure 4.** Optimized online SPE–ICP–MS–DRC profiles of  $^{99}\text{Tc}$ . Experimental conditions: sample, 50 mL of 0–0.5 ng/L  $^{99}\text{Tc}$  solution dissolved in 0.7 M  $\text{HNO}_3$ , DRC;  $\text{O}_2$  gas, 1.5 mL/min, detected ion, 99. The background (BL) is equivalent to the concentration 71.5 pg/L (45 mBq/L) of  $^{99}\text{Tc}$ .

using the proposed online SPE–DRC–ICP–MS system, which combines the TK201 online SPE and  $\text{O}_2$ -DRC. These peaks appeared at a retention time (RT) of 194 s, which was constant despite the changing concentration of  $^{99}\text{Tc}$  and/or coexistence of Mo and Ru. The elution of the peak tail ended at 366 s, and the analytical time for all of the samples was 24 min. The time depended on the sample volume; a majority of the time was consumed in the process of the SPE preconcentration rather than ICP–MS measurement. All experiments were conducted by injecting 50 mL of sample

volume to maintain a total analytical time of 24 min. The peak width was 4.3 min, denoting 8.5 mL of the eluate volume from the SPE (cf. eluate flow rate: 2.0 mL/min). This resulted in SPE preconcentration in which the sample volume (initial injection: 50 mL) was enhanced by 5.9 times. Peak height and peak area depended on the concentration of  $^{99}\text{Tc}$ , both of which exhibited a linear trend. For 50 mL of injected sample, the DL ( $3\sigma$ ) regarding the peak area was 9.3 pg/L (equal to 5.9 mBq/L) and the relative standard deviation (RSD) was 1.7% (50 mL of 0.2 ng/L  $^{99}\text{Tc}$ ;  $n = 3$ ). In addition, BEC and limit of quantification (LOQ) are 71.5 pg/L (45 mBq/L) and 30 pg/L (20 mBq/L), respectively.

The maximum allowances of coexistence (capable abundance) obtained by multiplying each part of the values were  $1.5 \times 10^{-13}$  (online SPE and DRC) and  $1.1 \times 10^{-5}$  (online SPE and mathematical correction) for  $^{99}\text{Tc}/\text{Mo}$  and  $^{99}\text{Tc}/\text{Ru}$ , respectively (shown in Table 1).

**Additional Offline Preconcentration: Anion-Exchange Preconcentration (IC).** Presently, typical ICP–MS techniques for  $^{99}\text{Tc}$  use additional preconcentration methods to enhance the amount of  $^{99}\text{Tc}$  because of its low concentration levels. The proposed method can be optionally used with offline preconcentration methods such as ion-exchange preconcentration (IC) and/or other additional SPE methods. In this study, 40.448 L of seawater was preconcentrated using AG1-X8 anion-exchange resin and prepared to a volume of 20.00 mL (i.e., volume ratio: 2022-fold), and the initial concentrations of Re (as a tracer), Mo, and Ru in the seawater were 10.1, 10.2, and 0.53  $\mu\text{g/L}$ , respectively. The recovery rates ( $R\%$ ) of Re (a tracer of  $^{99}\text{Tc}$ ), Mo, and Ru were 55.1, 1.21, and 3.00%, respectively. These values for Mo and Ru were  $4.5 \times 10^{-3}$  and  $3.6 \times 10^{-3}$ , i.e.,  $^{99}\text{Tc}/\text{Mo}$  and  $^{99}\text{Tc}/\text{Ru}$ , respectively.

The resulting coexistence in the entire system can theoretically be allowed to decrease to  $2.1 \times 10^{-14}$  and  $6.9 \times 10^{-6}$  for  $^{99}\text{Tc}/\text{Mo}$  and  $^{99}\text{Tc}/\text{Ru}$ , respectively. When using additional preconcentration methods, the DL<sub>total</sub> ( $3\sigma$ ) was 70.0 fg/L (the DL value was improved 1114-times greater than the single use of the online method of DL (10 mL sample injection): 78.0 pg/L). In addition, this value is approximately 1000 times greater than that enabled by methods of coexistence. Using this IC, an additional 9 h of analytical time was required (entire time of analysis: 10 h).

The final concentrations of Mo and Ru determined after IC preconcentration were 248.1 and 31.6  $\mu\text{g/L}$ , respectively. Although the proposed system (online SPE–ICP–MS–DRC) has the ability to achieve abundance values of  $1.5 \times 10^{-13}$  and  $1.1 \times 10^{-5}$  for  $^{99}\text{Tc}/\text{Mo}$  and  $^{99}\text{Tc}/\text{Ru}$ , respectively, the actual abundances after the IC preconcentration were  $4.0 \times 10^{-5}$  and  $3.2 \times 10^{-4}$  for  $^{99}\text{Tc}/\text{Mo}$  and  $^{99}\text{Tc}/\text{Ru}$ , respectively. Considering these values, the maximum preconcentration factor of seawater would be  $3.2 \times 10^3$  times, and its initial maximum volume can reach values of  $1.18 \times 10^3$  L (with preconcentrates down to 20 mL).

Alternatively, a large-volume auto-preconcentration method for  $^{99}\text{Tc}$ <sup>25</sup> or a high-performance separator<sup>63</sup> can be employed in the condition of less than the abundance ratio. Previously, Shi<sup>25</sup> reported that a large-volume auto-preconcentration method can achieve preconcentration from 200 L to several mL while maintaining an abundance ratio of  $10^{-5}$ – $10^{-7}$  for  $^{99}\text{Tc}/\text{Mo}$  and  $^{99}\text{Tc}/\text{Ru}$ ; such approaches are compelling means to improve sensitivity.



Table 1. Abundance Ratio of  $^{99}\text{Tc}/\text{Mo}$  and  $^{99}\text{Tc}/\text{Ru}$  at Each Separation Step

separation step	allowance coexistence ratio	
	$^{99}\text{Tc}/\text{Mo}$	$^{99}\text{Tc}/\text{Ru}$
online SPE	$2.9 \times 10^{-4}$	$2.2 \times 10^{-4}$
DRC with $\text{O}_2$	$5.0 \times 10^{-10}$	
mathematical correction		$5.0 \times 10^{-2}$
online ICP–MS–DRC	$1.5 \times 10^{-13}$	$1.1 \times 10^{-5}$
offline preconcentration	$4.0 \times 10^{-5}$	$3.2 \times 10^{-4}$
offline preconcentration + online ICP–MS–DRC	$5.8 \times 10^{-18}$	$3.5 \times 10^{-9}$

**Comparison with Other Methods.** When compared with existing techniques, the online SPE–ICP–MS–DRC technique proposed herein exhibits superior characteristics in terms of DL and required sample volume, as shown in Table S4 in the SI. The proposed method has the lowest DL of the online methods in the list. Most existing methodologies for  $^{99}\text{Tc}$  analysis using ICP–MS use the TEVA resin; therefore, manual handling is necessary during analysis and sample applications are limited. For example, seawaters have extremely low values of  $^{99}\text{Tc}/\text{Mo}$  and/or  $^{99}\text{Tc}/\text{Ru}$ . Furthermore, low values of  $^{99}\text{Tc}/\text{Mo}$  and/or  $^{99}\text{Tc}/\text{Ru}$  mean that it is difficult to increase the initial volume of the sample. Based on these comparisons, online SPE–ICP–MS–DRC should be the method of choice for  $^{99}\text{Tc}$  quantification, especially when considering measurements of environmental samples.

**Measurement of Environmental Samples.** The proposed results for five  $^{99}\text{Tc}$ -spiked environmental samples containing a certificated reference sample (IAEA-443) are summarized in Table 1. Without any additional pretreatment or omitting matrix elements from these samples before analysis, their quantified  $^{99}\text{Tc}$  values agreed well with the spiked numbers. Concentrations of Mo and Ru in the environmental samples measured via ICP–MS (normal) with dilution ( $10^0$ – $10^4$ ) using the  $\text{HNO}_3$  solution were 0.39, 0.015, 14.8, and 9.8  $\mu\text{g}/\text{L}$  for Mo in river water, groundwater, deep pond mineral water, and seawater, respectively. In contrast, concentrations of Ru were ND ( $<0.67$ ), 1.6, 11.1, and 1313  $\text{ng}/\text{L}$  for river water, groundwater, deep pond mineral water, and seawater, respectively. This gives  $^{99}\text{Tc}/\text{Mo}$  and  $^{99}\text{Tc}/\text{Ru}$  values of  $6.8 \times 10^{-5}$ – $6.7 \times 10^{-2}$  and  $7.6 \times 10^{-4}$ – $1.5 \times 10^0$ , respectively. The resulting  $^{99}\text{Tc}$  concentrations are significantly higher than those of Mo and Ru (approx. 6 and 3 orders of magnitude for Mo and Ru, respectively). In addition, the certificated reference material (IAEA-443 seawater) containing 0.159–0.250  $\text{mBq}/\text{kg}$  of  $^{99}\text{Tc}$  was measured by this method, and the resultant value significantly corresponded, as shown in Table 2.

This study also used condensed seawater samples with additional IC preconcentration to achieve a 2000-times enhancement of  $^{99}\text{Tc}$  sensitivity (40–20 mL). Among these experiments, aliquot volumes (10 mL), including  $^{99}\text{Tc}$  (100 pg), were directly injected into the system without any further preparation.  $R\%$  was 55.1% (Re tracer), and the DL of  $^{99}\text{Tc}$  was 70.0  $\text{fg}/\text{L}$  (44.3  $\mu\text{Bq}/\text{L}$ ). The concentration of nonspiked and spiked samples showed values below the DL (70.0  $\text{fg}/\text{L}$ ) and 111 pg (70.3  $\text{mBq}$ ), respectively. The use of additional (optional) pretreatment methods such as IC resin separation prior to online SPE–ICP–MS–DRC analysis did not preclude the quantification of  $\text{fg}/\text{L}$   $^{99}\text{Tc}$  concentrations.

Table 2.  $^{99}\text{Tc}$ -Spike and Recovery Test Results for Environmental Samples

sample <sup>a</sup>	addition/pg (mBq)	online SPE–ICP–MS–DRC/pg (mBq) <sup>b</sup>
river water	0.00	ND <sup>c</sup>
	10.0 (6.33) <sup>d</sup>	$9.84 \pm 0.53$ ( $6.23 \pm 0.33$ )
groundwater	0.00	ND <sup>c</sup>
	10.0 (6.33) <sup>d</sup>	$8.92 \pm 0.16$ ( $5.65 \pm 0.10$ )
deep pond mineral water	0.00	ND <sup>c</sup>
	10.0 (6.33) <sup>d</sup>	$9.94 \pm 0.20$ ( $6.29 \pm 0.13$ )
seawater	0.00	ND <sup>c</sup>
	10.0 (6.33) <sup>d</sup>	$8.85 \pm 0.92$ ( $5.60 \pm 0.58$ )
seawater (IAEA-443)	12.6–19.8 <sup>e</sup> (8.0–12.5) <sup>e</sup>	$15.81 \pm 0.76$ ( $10.00 \pm 0.48$ )

<sup>a</sup>All samples were prepared using a 0.7 M  $\text{HNO}_3$  solution. <sup>b</sup> $n = 3$ ; all samples (50.0 mL) were directly injected into the online SPE–ICP–MS–DRC without any additional preconcentration. <sup>c</sup>ND: non-detection ( $<9.3$   $\text{pg}/\text{L}$ ; equal to 0.465  $\text{pg}$  for 50 mL). <sup>d</sup>Total volume 50 mL (i.e., 0.2  $\text{ng}/\text{L}$ ). <sup>e</sup>Certificated concentration. The reported range is 0.251–0.395  $\text{ng}/\text{L}$  (0.159–0.250  $\text{mBq}/\text{kg}$ ).<sup>64</sup>

## CONCLUSIONS

In this study, the direct quantification of  $^{99}\text{Tc}$  in small aliquot volumes (50 mL) of environmental samples containing picogram levels of  $^{99}\text{Tc}$  was presented using online ICP–MS–DRC. Although  $^{99}\text{Tc}$  analyses using ICP–MS generally get disturbed in the presence of Mo and Ru, the combination of SPE, DRC, and QMS filter techniques allowed the coexistence of abundance ratios of  $1.5 \times 10^{-13}$  and  $1.1 \times 10^{-5}$  for  $^{99}\text{Tc}/\text{Mo}$  and  $^{99}\text{Tc}/\text{Ru}$ , respectively. Neither chemical separation nor manual handling was required to remove isobaric interferences from Ru and Mo during the measurement sequence. Background  $^{99}\text{Tc}$  noise signals were effectively suppressed via a thorough investigation of their noise sources. As most existing methodologies of  $^{99}\text{Tc}$  analysis do not allow the measurement of ultralow abundance ( $^{99}\text{Tc}/\text{Mo}$  and  $^{99}\text{Tc}/\text{Ru}$ ), it was difficult to analyze seawater samples. When investigating DRC, both optimization of the measurement and the removed species of Mo were considered. Under optimized conditions, a small volume of aliquot (50 mL) containing picogram concentrations of  $^{99}\text{Tc}$  was successfully analyzed using the proposed online ICP–MS–DRC method even in the presence of  $10^{11}$  or  $10^3$  times greater Mo and Ru interference sources. In many previous reports, significant interference has been ignored. Herein, we achieved the measurement of ultralow abundances ( $^{99}\text{Tc}/\text{Mo}$  and  $^{99}\text{Tc}/\text{Ru}$ ) using the proposed method, thus showing that it can be applied to large-volume preconcentrations. Environmental samples, such as river water, groundwater, deep pond mineral water, and seawater, can be analyzed within 24 min using this method.

Indeed, direct analysis using this method, as well as a combination of additional preconcentration, is applicable. The proposed method is a new and effective analytical methodology for rapid and trace analysis of  $^{99}\text{Tc}$  in environmental samples. It is particularly useful for distinguishing the very low abundances between  $^{99}\text{Tc}$  and potential interference (i.e., from  $^{99}\text{Tc}/\text{Mo}$  and  $^{99}\text{Tc}/\text{Ru}$ ) and is thus useful in the field of environmental radioactivity monitoring.

## ■ ASSOCIATED CONTENT

### Supporting Information

The Supporting Information is available free of charge at <https://pubs.acs.org/doi/10.1021/acsomega.1c02756>.

$^{99}\text{Tc}$ , Mo, and Ru concentrations in water samples (Table S1); parameters of online SPE–ICP–MS–DRC measurement (Table S2); flowchart of stepwise control of valve switching (Table S3); comparison of the recovery ( $R\%$ ) of 65 elements on the commercial SPE resins (Figure S1); adsorption and isolation property of  $^{99}\text{Tc}$  using TK201 resin with the double-column inline style (Figure S2); behaviors of  $^{98}\text{Mo}$ ,  $^{98}\text{Mo}^1\text{H}$ , and  $^{99}\text{Tc}$  with various types of gases in DRC (Figure S3); comparison of  $\text{O}_2$  effects in DRC for  $^{99}\text{Tc}$  and  $^{99}\text{Ru}$  (Figure S4); and comparison of analytical performance with other reported methods (Table S4) (PDF)

## ■ AUTHOR INFORMATION

### Corresponding Authors

**Makoto Matsueda** – Faculty of Symbiotic Systems Science, Cluster of Science and Technology, Fukushima University, Fukushima 960-1296, Japan; Collaborative Laboratories for Advanced Decommissioning Science, Japan Atomic Energy Agency, Fukushima 963-7700, Japan; Email: [matsueda.makoto@jaea.go.jp](mailto:matsueda.makoto@jaea.go.jp)

**Yoshitaka Takagai** – Faculty of Symbiotic Systems Science, Cluster of Science and Technology, Fukushima University, Fukushima 960-1296, Japan; Institute of Environmental Radioactivity, Fukushima University, Fukushima 960-1296, Japan; [orcid.org/0000-0002-7760-5636](https://orcid.org/0000-0002-7760-5636); Email: [s015@ipc.fukushima-u.ac.jp](mailto:s015@ipc.fukushima-u.ac.jp)

### Authors

**Kayo Yanagisawa** – Faculty of Symbiotic Systems Science, Cluster of Science and Technology, Fukushima University, Fukushima 960-1296, Japan

**Kazuma Koarai** – Collaborative Laboratories for Advanced Decommissioning Science, Japan Atomic Energy Agency, Fukushima 963-7700, Japan

**Motoki Terashima** – Collaborative Laboratories for Advanced Decommissioning Science, Japan Atomic Energy Agency, Fukushima 963-7700, Japan

**Kenso Fujiwara** – Collaborative Laboratories for Advanced Decommissioning Science, Japan Atomic Energy Agency, Fukushima 963-7700, Japan

**Hironobu Abe** – Collaborative Laboratories for Advanced Decommissioning Science, Japan Atomic Energy Agency, Fukushima 963-7700, Japan

**Akihiro Kitamura** – Collaborative Laboratories for Advanced Decommissioning Science, Japan Atomic Energy Agency, Fukushima 963-7700, Japan; Present Address: Naraha Center for Remote Control Technology Development, Sector of Fukushima Research and Development, Japan

Atomic Energy Agency (JAEA), 1-22 Nakamaru, Yamadaoka, Naraha, Fukushima 979-0513, Japan

Complete contact information is available at: <https://pubs.acs.org/10.1021/acsomega.1c02756>

## Author Contributions

M.M.: conceptualization, all experiments, and writing original draft. K.Y. and K.K.: a part of ICP–MS experiment. M.T., K.F., H.A., and A.K.: discussion. Y.T.: discussion, writing, editing, reviewing, methodology, and supervision.

## Notes

The authors declare no competing financial interest.

## ■ ACKNOWLEDGMENTS

The authors gratefully acknowledge funding from the JAEA Nuclear Energy S&T and Human Resource Development Project through a concentrating wisdom (Grant Number JPJA19H19210081).

## ■ REFERENCES

- (1) Riley, J. P.; Siddiqui, S. A. The Determination of Technetium-99 in Seawater and Marine Algae. *Anal. Chim. Acta* **1982**, *139*, 167–176.
- (2) Harvey, B. R.; Ibbett, R. D.; Williams, K. J.; Lovett, M. B. The Determination of Technetium-99 in Environmental Materials. *Fish. Res.* **1991**, *22*.
- (3) Chiu, J. H.; Chu, T. C.; Weng, P. S. Radiochemical Determination of Technetium-99 in LLW by Chelation with Sodium Diethyl Dithiocarbamate (NaDDC) and Extraction with Chloroform. *J. Radioanal. Nucl. Chem. Artic.* **1991**, *150*, 493–507.
- (4) Wigley, F.; Warwick, P. E.; Croudace, I. W.; Caborn, J.; Sanchez, A. L. Optimised Method for the Routine Determination of Technetium-99 in Environmental Samples by Liquid Scintillation Counting. *Anal. Chim. Acta* **1999**, *380*, 73–82.
- (5) Chen, Q.; Dahlgard, H.; Nielsen, S. P. Determination of  $^{99}\text{Tc}$  in Sea Water at Ultra Low Levels. *Anal. Chim. Acta* **1994**, *285*, 177–180.
- (6) Darab, J. G.; Smith, P. A. Chemistry of Technetium and Rhenium Species during Low-Level Radioactive Waste Vitrification. *Chem. Mater.* **1996**, *8*, 1004–1021.
- (7) Icenhower, J. P.; Qafoku, N. P.; Zachara, J. M.; Martin, W. J. The Biogeochemistry of Technetium: A Review of the Behavior of an Artificial Element in the Natural Environment. *Am. J. Sci.* **2010**, *310*, 721–752.
- (8) Shi, K.; Hou, X.; Roos, P.; Wu, W. Determination of Technetium-99 in Environmental Samples: A Review. *Anal. Chim. Acta* **2012**, *709*, 1–20.
- (9) Centre for Environment Fisheries and Aquaculture Science. *Radioactivity in Food and the Environment 2019: RIFE 25*.
- (10) García-León, M.  $^{99}\text{Tc}$  in the Environment: Sources, Distribution and Methods. *J. Nucl. Radiochem. Sci.* **2005**, *6*, 253–259.
- (11) Sellafield Ltd. *Monitoring Our Environment - Discharges and Environmental Monitoring*. Annual Report, 2019.
- (12) U.S. Department of Energy Assistant Secretary for Environmental Management. *Hanford Site Groundwater Monitoring Report for 2019*.
- (13) World Health Organisation. *Guidelines for Drinking-Water Quality*, 4th ed.; World Health Organisation: Geneva, 2017.
- (14) United States Environmental Protection Agency. *Radionuclides in Drinking Water: A Small Entity Compliance Guide*.
- (15) O'Hara, M. J.; Burge, S. R.; Grate, J. W. Quantification of Technetium-99 in Complex Groundwater Matrixes Using a Radiometric Preconcentrating Minicolumn Sensor in an Equilibration-Based Sensing Approach. *Anal. Chem.* **2009**, *81*, 1068–1078.
- (16) Hou, X.; Roos, P. Critical Comparison of Radiometric and Mass Spectrometric Methods for the Determination of Radionuclides in Environmental, Biological and Nuclear Waste Samples. *Anal. Chim. Acta* **2008**, *608*, 105–139.



- (17) Keith-Roach, M. J.; Stürup, S.; Oughton, D. H.; Dahlgard, H. Comparison of Two ICP-MS Set-Ups for Measuring  $^{99}\text{Tc}$  in Large Volume Water Samples. *Analyst* **2002**, *127*, 70–75.
- (18) Roos, P. Analysis of Radionuclides Using ICP-MS. *Radioact. Environ.* **2008**, *11*, 295–330.
- (19) Sahli, H.; Röllin, S.; Corcho Alvarado, J. A. Determination of  $^{99}\text{Tc}$  in Environmental Samples and Depleted Uranium Penetrators Using ICP-MS. *J. Radioanal. Nucl. Chem.* **2017**, *311*, 1633–1642.
- (20) Lehto, J.; Hou, X. J. *Chemistry and Analysis of Radionuclides*; Wiley-VCH Verlag GmbH & Co. KGaA: Weinheim, 2011; p 348.
- (21) Thomas, R. *Practical Guide to ICP-MS: A Tutorial for Beginners*, 3rd ed.; CRC Press: New York, 2013; p 53, 136–138.
- (22) Smedley, P. L.; Kinniburgh, D. G. Molybdenum in Natural Waters: A Review of Occurrence, Distributions and Controls. *Appl. Geochem.* **2017**, *84*, 387–432.
- (23) Stetzenbach, K. J.; Amano, M.; Kremer, D. K.; Hodge, V. F. Testing the Limits of ICP-MS: Determination of Trace Elements in Ground Water at the Part-Per-Trillion Level. *Groundwater* **1994**, *32*, 976–985.
- (24) Bekov, G. I.; Letokhov, V. S.; Radaev, V. N.; Baturin, G. N.; Egorov, A. S.; Kursky, A. N.; Narseyev, V. A. Ruthenium in the Ocean. *Nature* **1984**, *312*, 748–750.
- (25) Shi, K.; Qiao, J.; Wu, W.; Roos, P.; Hou, X. Rapid Determination of Technetium-99 in Large Volume Seawater Samples Using Sequential Injection Extraction Chromatographic Separation and ICP-MS Measurement. *Anal. Chem.* **2012**, *84*, 6783–6789.
- (26) Walas, S.; Kleszcz, K.; Tobiasz, A.; Mrowiec, H.; Mielinski, J. W. Determination of Technetium-99 in Peat by Flow Injection–Inductively Coupled Plasma Mass Spectrometry. *Anal. Lett.* **2016**, *49*, 2755–2765.
- (27) Kołacińska, K.; Samczyński, Z.; Dudek, J.; Bojanowska-Czajka, A.; Trojanowicz, M. A Comparison Study on the Use of Dowex 1 and TEVA-Resin in Determination of  $^{99}\text{Tc}$  in Environmental and Nuclear Coolant Samples in a SIA System with ICP-MS Detection. *Talanta* **2018**, *184*, 527–536.
- (28) Eroglu, A. E.; McLeod, C. W.; Leonard, K. S.; McCubbin, D. Determination of Technetium in Seawater Using Ion Exchange and Inductively Coupled Plasma Mass Spectrometry with Ultrasonic Nebulization. *Spectrochim. Acta, Part B* **1998**, *53*, 1221–1233.
- (29) Rodríguez, R.; Leal, L.; Miranda, S.; Ferrer, L.; Avivar, J.; García, A.; Cerdà, V. Automation of  $^{99}\text{Tc}$  Extraction by LOV Prior ICP-MS Detection: Application to Environmental Samples. *Talanta* **2015**, *133*, 88–93.
- (30) Wu, H. C.; Su, T. Y.; Tsai, T. L.; Jong, S. B.; Yang, M. H.; Tyan, Y. C. Rapid Determination of Technetium-99 by Automatic Solid Phase Extraction and Inductively Coupled Plasma Mass Spectrometry. *RSC Adv.* **2014**, *4*, 39226–39230.
- (31) Das, D.; Dutta, M.; Cervera, M. L.; de la Guardia, M. Recent Advances in On-Line Solid-Phase Pre-Concentration for Inductively-Coupled Plasma Techniques for Determination of Mineral Elements. *TrAC, Trends Anal. Chem.* **2012**, *33*, 35–45.
- (32) Liang, P.; Qin, Y.; Hu, B.; Peng, T.; Jiang, Z. Nanometer-Size Titanium Dioxide Microcolumn on-Line Preconcentration of Trace Metals and Their Determination by Inductively Coupled Plasma Atomic Emission Spectrometry in Water. *Anal. Chim. Acta* **2001**, *440*, 207–213.
- (33) Takagai, Y.; Furukawa, M.; Kameo, Y.; Suzuki, K. Sequential Inductively Coupled Plasma Quadrupole Mass-Spectrometric Quantification of Radioactive Strontium-90 Incorporating Cascade Separation Steps for Radioactive Contamination Rapid Survey. *Anal. Methods* **2014**, *6*, 355–362.
- (34) Furukawa, M.; Takagai, Y. Split Flow Online Solid-Phase Extraction Coupled with Inductively Coupled Plasma Mass Spectrometry System for One-Shot Data Acquisition of Quantification and Recovery Efficiency. *Anal. Chem.* **2016**, *88*, 9397–9402.
- (35) Ayala, A.; Takagai, Y. Sequential Injection Analysis System Exploiting On-Line Solid-Phase Extraction for the Determination of Strontium and Nickel by Microwave Plasma Atomic Emission Spectrometry. *Anal. Sci.* **2018**, *34*, 387–390.
- (36) Furukawa, M.; Matsueda, M.; Takagai, Y. Ultrasonic Mist Generation Assist Argon–Nitrogen Mix Gas Effect on Radioactive Strontium Quantification by Online Solid-Phase Extraction with Inductively Coupled Plasma Mass Spectrometry. *Anal. Sci.* **2018**, *34*, 471–476.
- (37) Furukawa, M.; Takagai, Y.; Matsunami, H.; Komatsuzaki, Y.; Kawakami, T.; Shinano, T.; Takagai, Y. Rapid Quantification of Radioactive Strontium-90 in Fresh Foods via Online Solid-Phase Extraction–Inductively Coupled Plasma–Dynamic Reaction Cell–Mass Spectrometry and Its Comparative Evaluation with Conventional Radiometry. *ACS Omega* **2019**, *4*, 11276–11284.
- (38) Yanagisawa, K.; Matsueda, M.; Furukawa, M.; Takagai, Y. Development of Online Dilution System for Quantification of  $^{90}\text{Sr}$  Using Automatic Solid-Phase Extraction Inductively Coupled Plasma Mass Spectrometry. *Anal. Sci.* **2020**, *36*, 1131–1135.
- (39) Kołacińska, K.; Chajduk, E.; Dudek, J.; Samczyński, Z.; Łokas, E.; Bojanowska-Czajka, A.; Trojanowicz, M. Automation of Sample Processing for ICP-MS Determination of  $^{90}\text{Sr}$  Radionuclide at ppq Level for Nuclear Technology and Environmental Purposes. *Talanta* **2017**, *169*, 216–226.
- (40) Vilas, V. V.; Millet, S.; Sandow, M.; Pérez, L. I.; Serrano-Purroy, D.; van Winckel, S.; de las Heras, L. A. An Automated Seafast ICP-DRC-MS Method for the Determination of  $^{90}\text{Sr}$  in Spent Nuclear Fuel Leachates. *Molecules* **2020**, *25*, No. 1429.
- (41) Kim, H.; Kang, Y. G.; Lee, Y. J.; Choi, S. D.; Lim, J. M.; Lee, J. H. Automated Extraction Chromatographic Radionuclide Separation System for Analysis of  $^{90}\text{Sr}$  in Seawater. *Talanta* **2020**, *217*, No. 121055.
- (42) Wang, W.; Evans, R. D.; Newman, K.; Khokhar, R. Automated Separation, Preconcentration and Measurement of  $^{90}\text{Sr}$  in Liquid Samples with Complex Matrices by Online Ion Exchange Chromatography Coupled with Inductively Coupled Plasma Mass Spectrometry (ICP-MS). *Talanta* **2021**, *222*, No. 121488.
- (43) Ceballos, M. R.; García-Tenorio, R.; Estela, J. M.; Cerdà, V.; Ferrer, L. An Integrated Automatic System to Evaluate U and Th Dynamic Lixiviation from Solid Matrices, and to Extract/Pre-Concentrate Leached Analytes Previous ICP-MS Detection. *Talanta* **2017**, *175*, 507–513.
- (44) Arnquist, I. J.; di Vacri, M. L.; Hoppe, E. W. An Automated Ultraclean Ion Exchange Separation Method for the Determinations of  $^{232}\text{Th}$  and  $^{238}\text{U}$  in Copper Using Inductively Coupled Plasma Mass Spectrometry. *Nucl. Instrum. Methods Phys. Res., Sect. A* **2020**, *965*, No. 163761.
- (45) Xiao, G.; Jones, R. L. Determination of  $^{239}\text{Pu}$  in Urine by Sector Field Inductively Coupled Plasma Mass Spectrometry (SF-ICP-MS) Using an Automated Offline Sample Preparation Technique. *J. Radioanal. Nucl. Chem.* **2021**, 277–287.
- (46) Avivar, J.; Ferrer, L.; Casas, M.; Cerdà, V. Fully Automated Lab-on-Valve-Multisyringe Flow Injection Analysis-ICP-MS System: An Effective Tool for Fast, Sensitive and Selective Determination of Thorium and Uranium at Environmental Levels Exploiting Solid Phase Extraction. *J. Anal. At. Spectrom.* **2012**, *27*, 327–334.
- (47) Qiao, J.; Hou, X.; Roos, P.; Miró, M. Rapid and Simultaneous Determination of Neptunium and Plutonium Isotopes in Environmental Samples by Extraction Chromatography Using Sequential Injection Analysis and ICP-MS. *J. Anal. At. Spectrom.* **2010**, *25*, 1769–1779.
- (48) Perna, L.; Betti, M.; Moreno, J. M. B.; Fuoco, R. Investigation on the Use of UTEVA as a Stationary Phase for Chromatographic Separation of Actinides On-Line to Inductively Coupled Plasma Mass Spectrometry. *J. Anal. At. Spectrom.* **2001**, *16*, 26–31.
- (49) Kim, C. K.; Kim, C. S.; Rho, B. H.; Lee, J. I. Rapid Determination of  $^{99}\text{Tc}$  in Environmental Samples by High Resolution ICP-MS Coupled with on-Line Flow Injection System. *J. Radioanal. Nucl. Chem.* **2002**, *252*, 421–427.
- (50) Shi, K.; Hou, X.; Roos, P.; Wu, W. Stability of Technetium and Decontamination from Ruthenium and Molybdenum in Determination of  $^{99}\text{Tc}$  in Environmental Solid Samples by ICPMS. *Anal. Chem.* **2012**, *84*, 2009–2016.

- (51) Mas, J. L.; García-León, M.; Bolívar, J. P.  $^{99}\text{Tc}$  Detection in Water Samples by ICP-MS. *Radiochim. Acta* **2004**, *92*, 39–46.
- (52) Chen, Q.; Dahlgard, H.; Hansen, H. J. M.; Aarkrog, A. Determination of  $^{99}\text{Tc}$  in Environmental Samples by Anion Exchange and Liquid-Liquid Extraction at Controlled Valency. *Anal. Chim. Acta* **1990**, *228*, 163–167.
- (53) Mas, J. L.; Tagami, K.; Uchida, S. Method for the Detection of Tc in Seaweed Samples Coupling the Use of Re as a Chemical Tracer and Isotope Dilution Inductively Coupled Plasma Mass Spectrometry. *Anal. Chim. Acta* **2004**, *509*, 83–88.
- (54) Triskem International (French). *TK201 Resin Product Sheet*.
- (55) Neubauer, K. R.; Knopp, M. A.; Davidowski, L.; Dionne, L. Trace Analyses in Metal Matrices Using the ELAN DRC II. *Appl. Note* **2019**, *100*, 1–8.
- (56) Amais, R. S.; Virgilio, A.; Schiavo, D.; Nóbrega, J. A. Tandem Mass Spectrometry (ICP-MS/MS) for Overcoming Molybdenum Oxide Interferences on Cd Determination in Milk. *Microchem. J.* **2015**, *120*, 64–68.
- (57) Sugiyama, N.; Nakano, K. Reaction Data for 70 Elements Using  $\text{O}_2$ ,  $\text{NH}_3$ , and  $\text{H}_2$  Gases with the Agilent 8800 Triple Quadrupole ICP-MS. *Agil. Technol. Appl. Note. P/NS990-4585EN*, 2014; pp 1–14.
- (58) Tanner, S. D.; Baranov, V. I.; Bandura, D. R. Reaction Cells and Collision Cells for ICP-MS: A Tutorial Review. *Spectrochim. Acta, Part B* **2002**, *57*, 1361–1452.
- (59) D'Ilio, S.; Violante, N.; Majorani, C.; Petrucci, F. Dynamic Reaction Cell ICP-MS for Determination of Total As, Cr, Se and V in Complex Matrices: Still a Challenge? A Review. *Anal. Chim. Acta* **2011**, *698*, 6–13.
- (60) Yamada, N. Kinetic Energy Discrimination in Collision/Reaction Cell ICP-MS: Theoretical Review of Principles and Limitations. *Spectrochim. Acta, Part B* **2015**, *110*, 31–44.
- (61) Martínez, A.; Köster, A. M.; Salahub, D. R. Reaction of a Mo Atom with  $\text{H}_2$ ,  $\text{N}_2$ , and  $\text{O}_2$ : A Density Functional Study. *J. Phys. Chem. A* **1997**, *101*, 1532–1541.
- (62) Koyanagi, G. K.; Caraiman, D.; Blagojevic, V.; Bohme, D. K. Gas-Phase Reactions of Transition-Metal Ions with Molecular Oxygen: Room-Temperature Kinetics and Periodicities in Reactivity. *J. Phys. Chem. A* **2002**, *106*, 4581–4590.
- (63) Chung, K. H.; Do Choi, S.; Choi, G. S.; Kang, M. J. Design and Performance of an Automated Radionuclide Separator: Its Application on the Determination of  $^{99}\text{Tc}$  in Groundwater. *Appl. Radiat. Isot.* **2013**, *81*, 57–61.
- (64) International Atomic Energy Agency. *Interlaboratory Comparison Radionuclides in Irish Sea Water - IAEA-443*.